a localization of absorption at the "surface" seems to be difficult to be understood physically, realizing that the C^{12} nucleus and the deuteron have a comparable size.

The final fit (Fig. 7) that has been obtained represents the general characteristics of the experimental data satisfactorily, especially when it is realized that both the optical model and the DWBA model appear not to be very good approximations for light nuclei. The main difference between the noncutoff DWBA and the experimental curve is the minimum near 33° that persists in all the theoretical curves. The fact that the cutoff DWBA curve fits the forward part of the angular distribution may very well indicate however that the inclusion of finite-range effects that tend to enhance the surface stripping contribution might improve the noncutoff fit in this region.

ACKNOWLEDGMENTS

We wish to express our gratitude to The Weizmann Institute of Science, in particular to the Department of Nuclear Physics, for its kind hospitality and to the Mathematical Department for placing at our disposal its excellent computing facilities.

We are very grateful to B. Krinsky for his programming work and continuous assistance which forms an essential contribution to this paper.

One of us (R.v.D.) greatly acknowledges the financial support of the Netherlands Organization for the Advancement of pure Research Z.W.O.

PHYSICAL REVIEW VOLUME 136, NUMBER 6B 21 DECEMBER 1964

$Li^7(Li^7,He^6)Be^8$ Reaction*

R. R. CARLSON, R. L. MCGRATH,† AND E. NORBECK
Department of Physics and Astronomy, University of Iowa, Iowa City, Iowa
(Received 7 August 1964)

Energy spectra of He^6 particles emitted in the nuclear reaction $Li^7(Li^7,He^6)Be^8$ were measured using a two-parameter E-dE/dx data-taking system which incorporated a general-purpose computer. Incident Li^7 ions had an energy of 3.0 MeV. The energy spectra showed peaks corresponding to the ground state and first (2.9 MeV) excited state of Be^8 and an anomalous yield between these states. This yield is simply explained as resulting from the two-step reaction $Li^7(Li^7,\alpha)Be^{10*}(He^6)\alpha$. No evidence for direct three-body breakup is found. He^6 angular distributions do not exhibit strong structure; the ground-state group shows slight anisotropy.

INTRODUCTION

THE $Li^7(Li^7,He^6)Be^8$ reaction is an exothermic ($Q=7.229$ MeV) reaction involving identical particles. The reaction mechanism is of interest because of the information this reaction might give about the nuclear wave functions. If the reaction proceeds by nucleon transfer via tunneling, reduced widths could be extracted from differential cross-section data. The plausibility of this reaction mechanism is enhanced in the present work because the incident kinetic energy is only 0.6 of the Coulomb barrier ($r=2.7$ F). One of the objectives of the present work was to obtain angular distribution data to make possible a test of the applicability of this reaction mechanism.

Transfer reactions have been studied before. The $Be^9(Le^7,Li^8)Be^8$ is a prime example.[1] An interpretation of the results of this study by barrier tunneling has had some success.[2] The $N^{14}(N^{14},N^{13})N^{15}$ reaction[3] is another example and theoretical interpretation of this reaction has had success.[4,5] In these cases, there is little energy release resulting from the rearrangement of nucleons compared to the incident kinetic energy. The $Li^7(Li^7,He^6)Be^8$ reaction, if it is a direct transfer reaction, is an example of tunneling where semiclassical approximations are precluded by the large Q value.

Several experiments providing energy spectra of the Be^8 nucleus have indicated an anomalous yield at about 1 MeV excitation in Be^8. This effect has been observed in the following reactions: $B^{11}(p,\alpha)Be^8$,[6] $Be^9(p,d)Be^8$,[7] and $Be^9(He^3,\alpha)Be^8$.[8] It has been attributed to the

* This research was supported in part by the National Science Foundation.

† Work performed while United States Steel Foundation Postgraduate Fellow 1963–1964.

[1] E. Norbeck, J. M. Blair, L. Pinsonneault, and R. J. Gerbracht, Phys. Rev. **116**, 1560 (1959).

[2] S. K. Allison, *Reactions Between Complex Nuclei* (John Wiley & Sons Inc., New York, 1960), p. 213.

[3] L. C. Becker, F. C. Jobes, and J. A. McIntyre, in *Proceedings of the Third International Conference on Reactions Between Complex Nuclei, Asilomar, 1963* (University of California Press, Berkeley, 1963). p. 106.

[4] K. R. Greider, Phys. Rev. **133**, B1483 (1964).

[5] Breit, Chin, and Wahrswerber, Phys. Rev. **133**, B404 (1964).

[6] E. H. Beckner, C. M. Jones, and G. C. Phillips, Phys. Rev. **123**, 255 (1961).

[7] See Ref. 6.

[8] J. A. Weinman and R. K. Smithers, Nucl. Phys. **45**, 260 (1963).

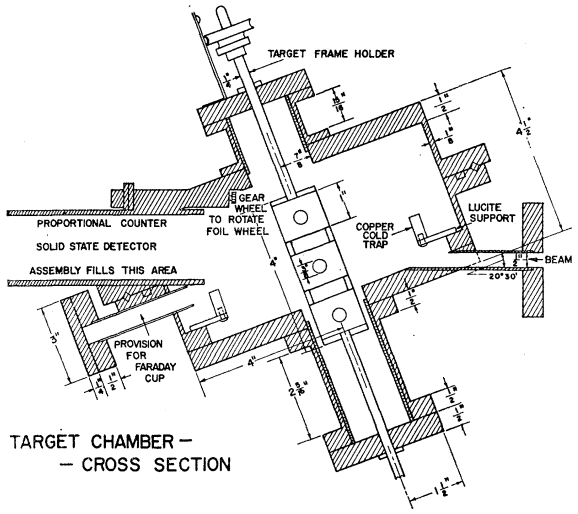

FIG. 1. Target-chamber cross section.

density-of-states function[9,10] of the Be^8 system which, apart from a delta function character at 0.095 MeV above the α-α threshold, has a maximum at about 1 MeV resulting from the rapid increase of the α-α penetrabilities above the threshold coupled with the less rapid change of the ground-state-resonance phase shift. This anomalous yield is predicted to have the same angular dependence as the ground state and a yield about 10% as large as the ground-state yield.[9] The $Li^7(Li^7,He^6)Be^8$ reaction provides another test of these predictions.

In order to cope with the variety of outgoing particles from the Li^7+Li^7 reaction, where exit channels with protons, deuterons, tritons, and alpha particles all have positive Q, a particle identification system was used. This was built around a general purpose computer which was also used to analyze data and make necessary calculations. Charged particles were stopped in a solid state detector which was located inside a proportional counter detector, and pulses from both detectors were simultaneously analyzed and then stored in two-parameter form.

EXPERIMENTAL PROCEDURE

The lithium ion beam is generated in the University of Iowa 4-MeV Van de Graaff accelerator. Momentum analysis and apertures define beam homogeneity to 0.5%; absolute beam energy is known to 2%.

The target chamber is shown in Fig. 1. The rotating detector is inclined 20.5 deg with respect to the chamber axis which is itself tilted 20.5 deg from the normal to the beam direction. Measurements from 0 to 139 deg in the laboratory may be made, although in this experiment He^6 could not be detected past 90 deg. A fixed n-p junction detector at 90 deg (lab) was used to normalize data.

Targets are prepared by evaporating enriched Li^7F on 0.7 mg/cm² Al foil. The Li^7F is about 200 keV thick to the 3 MeV lithium beam.

Since lithium-induced reactions have positive Q values for many charged particle exit channels, a particle identification system is necessary. The problem of resolving He^6 from He^4 is particularly acute because of typically large He^4 yields. For this reason, and because He^6 undergoes large energy loss in matter, the solid state E counter was mounted inside the proportional counter as shown in Fig. 2. The acceptance angle of the E detector was ± 3 deg. A 95% A, 5% CO_2

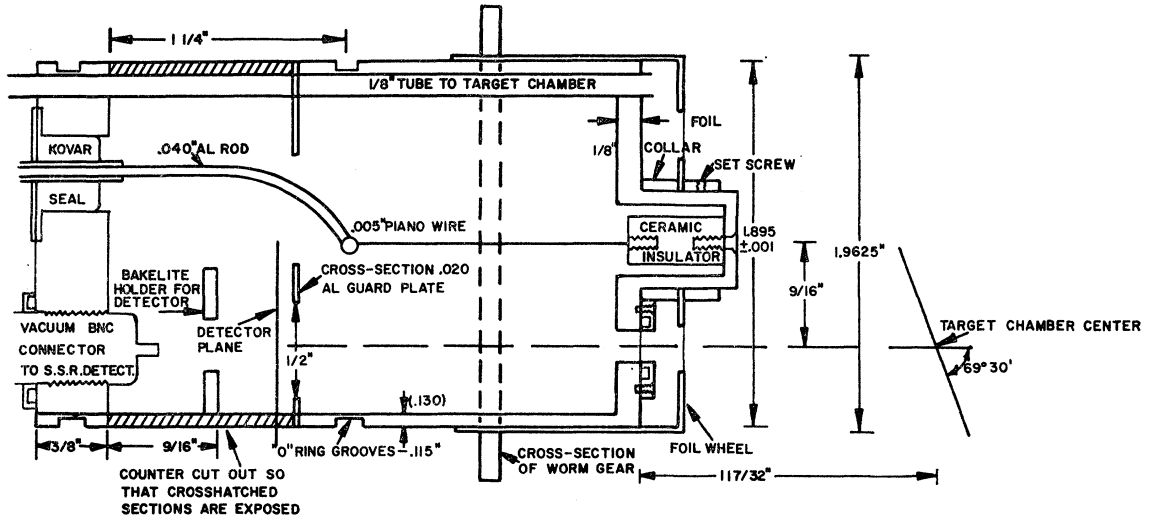

FIG. 2. E-dE/dx detector assembly cross section.

[9] F. C. Barker and P. B. Treacy, Nucl. Phys. 38, 33 (1962).
[10] G. C. Phillips, T. A. Griffy, and L. C. Biedenharn, Nucl. Phys. 21, 327 (1960).

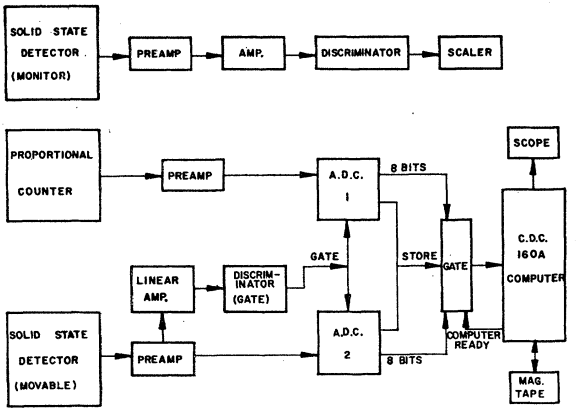

FIG. 3. Block diagram of electronics.

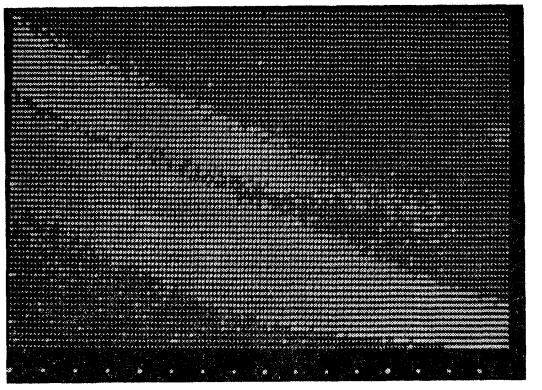

FIG. 4. Two-parameter E-dE/dx condensed oscilloscope display showing He^6, He^4 groups. Bright channels have four or more counts.

mixture was used in the proportional counter. Gas stopping power was measured with ThB decay alpha particles of known energy and was equivalent to 1.3 ± 0.1 mg/cm^2 Al. A 0.001-in. Mylar foil (equivalent to 0.9 ± 0.1 mg/cm^2 Al) covered the entrance aperture of the proportional counter. The minimum detectable He^6 energy was 4.0 MeV.

A block diagram of the electronics is given in Fig. 3. A Model 100-A Tennelec[11] preamplifier was used at the output of the E detector. The linear amplifiers and gate circuit are Sturrup Model 1402 components.[12] A multiparameter pulse-height analysis system designed by Carlson and Norbeck[13] analyzed the coincident E and ΔE pulses. Nuclear Data 160F analog to digital converters performed 256-channel pulse-height analysis on both input pulses simultaneously. Both eight-bit words containing the pulse-height information were then read into a Control Data 160-A computer which, in turn, wrote them on magnetic tape. In addition, a condensed 60×128 array of the ΔE versus E information was formed in the computer memory for oscilloscope display in two-parameter form. This display took place at the same time the data were collected and served to monitor the data collection.

The two-parameter E and ΔE data were subsequently analysed on the 160-A computer by scanning the magnetic tape and forming blocks of 60×128 out of the complete 256×256 array collected. The size of the block is determined by the computer memory size which is 64×128, and by the computer work length which was 12 bits. This word length allows storage of up to 4095 counts in each element of the block. Four out of the 64 rows in the memory were used for programs, leaving 60×128 places to set up a block out of the complete array. In an array such as this, where one has $\Delta E(60)$ along the one direction and $E(128)$ along the other, a particle type will fall into a particular region determined by the dependence of its ionization-energy loss rate on its energy. A particular particle type was defined so that the computer could recognize it by using a "light pen" to mark the regions in the block, presented in two-parameter form in an oscilloscope display, which corresponded to the particle type. A block of the total array is shown in Fig. 4 in the form of a contour map. Bright points correspond to places where four or more counts were collected. The higher band shows He^6 counts, the lower one He^4. The He^6 energy spectrum was obtained by using the particle identification programmed into the computer in this way to select pulse-height measurements according to particle type. In other words, the appropriate region was projected onto the E axis by summing counts in the ΔE direction, and displaying the sum at the corresponding value of E. This procedure was used to obtain both He^6 and He^4 energy spectra.

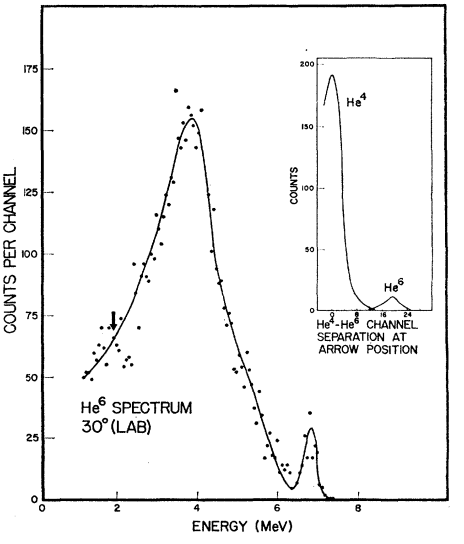

FIG. 5. He^6 energy spectrum in E detector at 30 deg (lab). The dE/dx cross section at position marked by arrow is shown in inset.

[11] Tennelec Instrument Co., P. O. Box 964, Oak Ridge, Tennessee.
[12] Sturrup, Inc., 50 Silver Street, Middletown, Connecticut.
[13] R. R. Carlson and E. Norbeck, Phys. Rev. **131**, 1204 (1963).

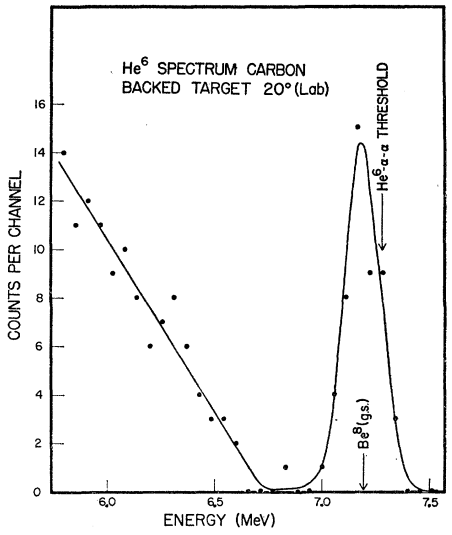

FIG. 6. He⁶ energy spectrum at 20 deg (lab) taken with thin target on carbon foil backing.

Figure 5 shows the measured He⁶ energy spectrum at 30 deg (lab). The inset is a profile in the ΔE direction at the E channel marked by the arrow. The He⁴, He⁶ groups show negligible overlap. The ratio of the He⁴ to He⁶ peak height is 15 to 1; the He⁶ peak to valley ratio is 10 to 1.

In order to study the details of the energy spectrum of the He⁶ particles in the neighborhood of the threshold for the $Li^7(Li^7, He^6)2\alpha$ reaction, measurements were made with a very thin (~20 keV to 3 MeV Li^7 ions) Li^7 target on a very thin carbon foil backing (~20 $\mu g/cm^2$). This target gave little yield and was useless on this account for angular distribution measurements, but it did produce a spectrum with better resolution in the threshold region. This region is shown in Fig. 6. Of particular interest is the very low valley in the Be⁸ excitation range just above the ground state peak.

Since data on He⁴ from the $Li^7(Li^7,\alpha)Be^{10}$ reaction are collected concurrently with that on He⁶, comparisons of relative cross sections may be made. A He⁴ spectrum at 50 deg (lab) is presented in Fig. 7. Four peaks are evident corresponding to unresolved levels in Be¹⁰ at 5.96, 6.18, and 6.26 MeV for one peak; at 7.37, 7.54 MeV for the second peak; at 9.27, 9.4 MeV for the third; and at 10.7 MeV for the fourth. The amplifier gain was set to spread the He⁶ spectrum over the pulse-height analyzer range so that He⁴ peaks corresponding to lower excited states in Be¹⁰ were beyond the analyzer range and were rejected. Energy release in the $Li^7(Li^7,\alpha)Be^{10}$ reaction is 14.771 MeV which is much larger than that in the $Li^7(Li^7,He^6)Be^8$ reaction.

Measurements were made at 10 deg intervals from 10 to 90 deg (lab). The target was oriented at 45 deg to the beam direction. He⁶ particles were detected through the target backing from 10 to 60 deg, and off the target face from 60 to 90 deg to reduce the amount of absorbing material because of the low He⁶ energy.

In order to check chamber symmetry the angular distribution of the $Li^7(Li^7,\alpha)Be^{10*}$ reaction was measured and found to agree with previous measurements.[14]

ENERGY SPECTRA

At each angle of observation spectra were corrected for energy loss in the target, target backing, proportional counter entrance window, and solid state detector dead layer (equivalent to 0.2 mg/cm² Al). At 30 deg the total amount of stopping material was equivalent to 3.4±0.1 mg/cm² of Al. He⁶ range-energy curves were constructed from He⁴ range-energy data[15] by assuming the He⁶ ionization energy loss equal to He⁴ at equal velocities. After these corrections were made, the peaks in the measured spectra were found to coincide with the expected positions of groups of He⁶ particles corresponding to the Be⁸ nucleus being left in its ground state and its first excited state at 2.9 MeV. The width of the ground state peak in Fig. 5 is caused by target thickness.

The differential cross section for the 2⁺, 2.9-MeV Be⁸ state was calculated using Barker and Treacy's[8] formulation:

$$\frac{d^2\sigma}{d\Omega_c dE_c} \sim E_c^{1/2}(P_2)^{-1}\sin^2\beta_2. \quad (1)$$

The symbols Ω_c and E_c refer to the center-of-mass solid angle and energy of the He⁶ particle. P_2 and β_2 are the α wave penetrability and resonance phase shifts of the α-α system. Values of P_2 were computed from published tables[16] (the α-α interaction radius was assumed to be 3.5 F) and β_2 values were taken from Barker and Treacy. $E_c^{1/2}$ is proportional to the outgoing He⁶ wave number and the remainder of the expression

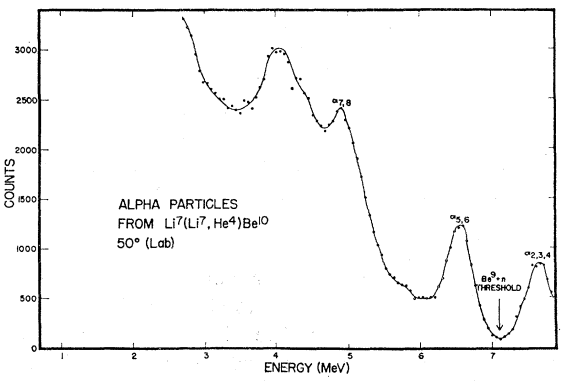

FIG. 7. He⁴ energy spectrum at 50 deg (lab).

[14] T. G. Dzuboy and J. M. Blair, Phys. Rev. 134, B586 (1964).
[15] W. Whaling, in *Handbuch der Physik*. edited by S. Flügge (Springer-Verlag, Berlin, 1958) Vol. 34, p. 193.
[16] W. T. Sharp, H. E. Gove, and E. B. Paul, Chalk River Project, 1955 (unpublished).

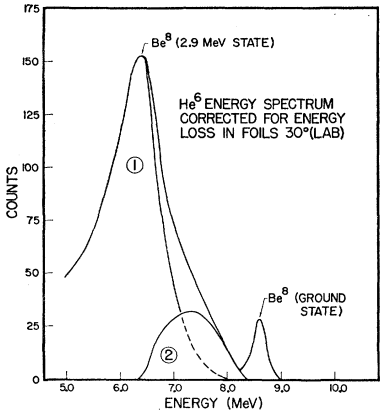

FIG. 8. He^6 energy spectrum at 30 deg corrected for energy loss in absorbing materials. Curve 1 represents the theoretical line shape of the 2.9 MeV Be^8 state. Curve 2 is the minimum anomalous yield.

is the density of states associated with the Be^8 nucleus. The expression above was transformed from the center-of-mass system to the laboratory system using the relation

$$\frac{d^2\sigma}{d\Omega dE}=\frac{\partial(E_c,\Omega_c)}{\partial(E,\Omega)}\frac{d^2\sigma}{d\Omega_c dE_c}, \tag{2}$$

where the Jacobian is determined by the kinematics of the reaction. The large width of the state implied by Eq. 1 means that different parts of the peak due to this state as seen in the laboratory correspond to different center-of-mass angles. The center-of-mass angle varies by 3.5 deg over the Be^8 excitation energy range from 0.8 to 4.5 MeV for a spectrum at 30 deg (lab). Possible angular dependence of $d^2\sigma/dE_c d\Omega_c$ over this range was ignored; the Jacobian angular dependence over this range is negligible. This transformed line shape is plotted in Fig. 8 and labeled curve 1.

Figure 8 shows the measured He^6 spectrum after energy loss corrections have been applied. Data were taken from Fig. 5. The calculated line shape of the 2.9-MeV state does not account for the observed peak shape. The excess yield is plotted as curve 2 in Fig. 8. Curve 2 represents a lower limit of anomalous yield; i.e., the curve is obtained by subtracting the 2.9-MeV peak shape with peak height equal to the experimental peak height. The real shape and magnitude of the anomalous yield is therefore probably not represented by curve 2. The anomaly is similar to the yields reported in other work.[6–8]

ANGULAR DISTRIBUTIONS

Figure 9 gives the result of two separate measurements of the angular distribution of the He^6 particles corresponding to 0^+, Be^8 ground state. The yield at each angle was taken as the number of counts under the ground state peak. The monitor counter was used to normalize runs. An even Legendre polynomial was fitted to the data by least squares, giving

$$\left(\frac{d\sigma}{d\Omega}\right)_{0^+}\sim(1.00\pm0.05)P_0+(0.12\pm0.10)P_2+(0.52\pm0.10)P_4. \tag{3}$$

Error estimates include statistical uncertainty only.

Angular distributions of yields corresponding to curves 1 and 2 of Fig. 8 are given in Fig. 10. Since the continuum shape may be angle-dependent, the division into yields corresponding to these curves may not be physically meaningful. Probable error estimates are based on statistical uncertainty. Both angular distributions are essentially isotropic.

DISCUSSION

(a) Energy Spectra

It has been shown above that a combination of the 2.9 MeV and ground states of Be^8 cannot fit the He^6 energy spectrum. Region 2 in Fig. 8 represents the minimum excess. The excess cannot be a "ghost" of the Be^8 ground state because the yield of the excess is at least 4 times larger than that of the ground state, instead of $\frac{1}{10}$ as predicted; nor can it be attributed to gamma decay of the 1.71-MeV He^6 state. It has been shown[17] both that the width of this state is less than 100 keV and that it decays via the $\alpha+n+n$ mode. There are several alternative explanations.

A three-body breakup filling the available phase space would give rise to a He^6 energy spectrum of the following form:

$$\frac{d\sigma}{dE_c d\Omega_c}\sim E_c^{1/2}\left(E_T-\frac{8E_c}{6}\right)^{1/2}. \tag{4}$$

E_T is the total energy available to the He^6-α-α system. The three-body spectrum would extrapolate to zero 94 keV above the ground state peak, and Fig. 8 shows

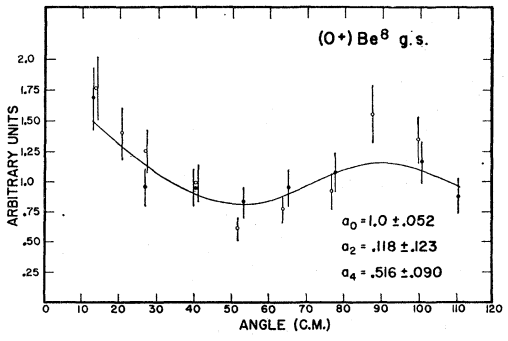

FIG. 9. Center-of-mass angular distributions of He^6 from the 0^+ ground state of Be^8. Due to particle identity in entrance channel, distribution is symmetric about 90 deg. Error bars represent statistical uncertainty only.

[17] K. W. Allen, E. Almqvist, J. T. Dewan, and T. P. Pepper, Phys. Rev. **96**, 684 (1954).

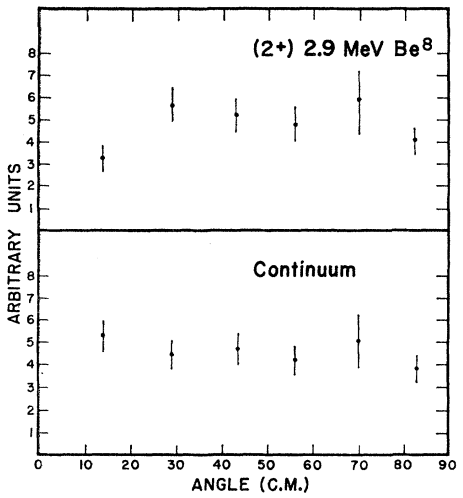

FIG. 10. Center-of-mass angular distributions of curves 1 and 2 in Fig. 8.

that this is not the case. The classical three-body phase space distribution in (4) would require yield of significant amounts in the valley between the ground-state peak and the 2.9-MeV state peak. In addition to the data in Fig. 8, the data in Fig. 6 rule out this explanation. The classical distribution may be modified by penetrabilities of the outgoing particles, however. Delves[18] has shown how such distortions arise where the three-body system has nonzero angular momentum. Very special assumptions would be required in this case, making the three-body breakup an unlikely explanation for the presence of the continuum.

The continuum could be due to the two-step reaction

$$\mathrm{Li}^7+\mathrm{Li}^7 \rightarrow \mathrm{Be}^{10*}+\alpha,$$
$$\mathrm{Be}^{10*} \rightarrow \mathrm{He}^6+\alpha.$$

If Be^{10} is excited to the 10.7-MeV state, then the kinematics of the reaction give the maximum He^6 energy to be 4.48 MeV in the center-of-mass system. The minimum energy is 0.073 MeV. If Be^{10} is excited to the 9.27-, 9.4-MeV states, then the maximum He^6 energy is 2.88 MeV and the minimum is 0.23 MeV. These maximum He^6 energies correspond to excitation energies in the Be^8 system of 0.92 MeV and 3.71 MeV in the case of a single-step two-body breakup. This would seem to explain the observed excess. Curve 2 in Fig. 8 implies a contribution from the 10.7-MeV state in Be^{10}. A similar explanation of the alpha particle spectrum of the $B^{11}(p,\alpha)Be^8$ has been given by Bethe.[19]

(b) Relative Cross Sections

The yield of He^6 (to an excitation of 4 MeV in Be^8) relative to the yield of the 5.96, 6.18, and 6.26 MeV Be^{10} was obtained by comparing He^6 and He^4 spectra at the same angles and integrating over angle. For the 2.9 MeV state of Be^8 the relative yield is 0.72 ± 0.20. For the continuum a lower limit corresponding to curve 2 in Fig. 8 for the relative yield is 0.17 ± 0.20. For the ground state of Be^8 the relative yield is 0.036 ± 0.01.

The above yields are not inconsistent with the hypothesis that the continuum is due to a two-step reaction through the 10.7-MeV Be^{10} state. The total He^4 yield to this state (see Fig. 7) is such that the yield represented by curve 2 in Fig. 8 implies a lower limit on the branching ratio of this state for decay into He^6+He^4 of about 7%.

The total cross section for formation of these Be^{10} states has been reported to be 4 ± 0.6 mb by Dzubay and Blair.[14] He^6 cross sections are therefore about 3 (upper limit) and 0.2 mb for formation of the 2.9 MeV and ground Be^8 states. These cross sections may be compared to that for the $Be^9(Li^7,Li^8)Be^8$ reaction, where Norbeck *et al.*[1] find 30 mb at 3.0-MeV lithium energy for formation of the ground and first excited Li^8 states. Presumably, the small neutron binding energy in Be^9 permits large cross sections for direct neutron pickup from the Be^9 nucleus.[2] The large proton binding energy in Li^7 evidently impedes direct proton transfer in the present experiment.

The ratio of twenty to one (upper limit) for formation of the 2.9 MeV and ground Be^8 levels is in part due to the $(2J_F+1)$ phase space factor. The remaining four to one ratio may be due to an underestimate of the continuum yield or to the character of the reaction mechanism for forming He^6+Be^8.

(c) Angular Distributions

The three distributions in Figs. 9 and 10 have little structure. If the continuum has no strong angular dependence, then the angular distribution of curve 1 represents that of the 2.9-MeV state. Interpretation of our results in terms of a reaction mechanism is difficult. The low bombarding energy and large Q value are expected to enhance direct reaction contributions to the cross section; however, the angular distributions do not exhibit the strong structure usually associated with this mechanism.

[18] L. M. Delves, Nucl. Phys. **20**, 257 (1960).

[19] H. A. Bethe, Rev. Mod. Phys. **9**, 69 (1937).

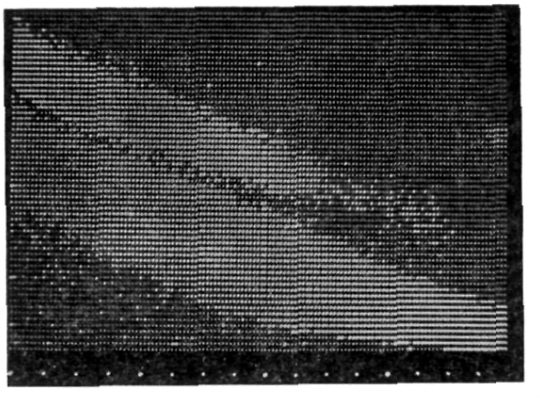

FIG. 4. Two-parameter E-dE/dx condensed oscilloscope display showing He^6, He^4 groups. Bright channels have four or more counts.